

Effect of the In-Plane Magnetic Field on Conduction of the Si-inversion Layer: Magnetic Field Driven Disorder

V. M. Pudalov^a, G. Brunthaler^b, A. Prinz^b, G. Bauer^b

^a *P. N. Lebedev Physics Institute, 117924 Moscow, Russia.*

^b *Institut für Halbleiterphysik, Johannes Kepler Universität, Linz, Austria*

We compare the effects of temperature, disorder and parallel magnetic field on the strength of the metallic-like temperature dependence of the resistivity. We found a similarity between the effects of disorder and parallel field: the parallel field weakens the metallic-like conduction in high mobility samples and make it similar to that for low-mobility samples. We found a smooth continuous effect of the in-plane field on conduction, without any threshold. While conduction remains non-activated, the parallel magnetic field restores the same resistivity value as the high temperature does. This matching sets substantial constraints on the choice of the theoretical models developed to explain the mechanism of the metallic conduction and parallel field magnetoresistance in 2D carrier systems. We demonstrate that the data for magneto- and temperature dependence of the resistivity of Si-MOS samples in parallel field may be well described by a simple mechanism of the magnetic field dependent disorder.

PACS: 71.30.+h, 73.40.Hm, 73.40.Qv

I. INTRODUCTION

The apparent metallic-like temperature dependence of the resistivity is observed in various two-dimensional (2D) carrier systems [1–8] and remains a focus of a broad interest because it challenges the conventional theory of the metallic conduction. The effect manifests itself in a strong drop of the resistivity over a limited range of temperatures, $T = (0.5 - 0.05)T_F$, from a high temperature value (call it ‘Drude’ value) $\rho_{\text{high}} = \rho(T \approx T_F)$ to a low temperature one $\rho_0 = \rho(T \lesssim 0.05T_F)$, here T_F is the Fermi temperature. Upon lowering the temperature further, a strong ‘metallic’ drop in ρ was found to cross over to the conventional weak localization type dependence [9–13]. Recently, it was demonstrated [11,13] that the ‘metallic’ drop is not related to quantum interference and in this sense should have a semiclassical origin.

Magnetic field applied in the plane of the 2D system causes a dramatic increase in resistivity [14–18]. It was proven experimentally [19,20] that the magnetoresistance (MR) in Si-MOS samples is mainly caused by spin-effects, though certain contribution of orbital effects [21] is noticeable at very large fields [20], bigger than the field of the spin polarization. The two effects, *strong metallic drop in resistivity* and *parallel field magnetoresistance* remain *puzzling*.

In this paper we demonstrate that (i) the strength of both effects is well matched and (ii) the action of magnetic field on conduction is similar to that of disorder and to some extent to that of temperature. In particular, in the presence of in-plane magnetic field the strong temperature dependence of the resistivity for a high mobility sample transforms into a weaker one and shifts to higher temperatures; both these features are typical for low mobility samples. Next, (iii) the effect of the magnetic field on the resistivity is continuous and shows no signatures of a threshold. Finally, (iv) increase in either temper-

ature or parallel magnetic field restores the same high-temperature (‘Drude’) resistivity value while transport remains non-activated. Matching of the actions of the above controlling parameters sets substantial constraints on the choice of theoretical models.

We performed measurements on a number of different mobility (100) n -Si-MOS samples, because this system demonstrates the most dramatic appearance of the discussed effects. Table I below shows the relevant parameters for the four most intensively studied samples whose mobilities differ by a factor of 25; parameters for other samples were reported in Refs. [3,9,13,22].

TABLE I. Relevant parameters of the five samples. μ_{peak} [m^2/Vs] is the peak mobility at $T = 0.3\text{K}$, ρ_c is in units of h/e^2 , and n_c is in 10^{11}cm^{-2} .

sample	μ_{peak}	n_c	ρ_c
Si 9	4.3	0.75	3.2
Si 15	4.0	0.88	2
Si 43	1.96	1.4	0.67
Si 39	0.51	3.5	0.32
Si 46	0.15	8.3	0.3

In Figures 1 a, c we plotted the temperature dependence of resistivity ρ for the highest and lowest mobility samples. At high carrier density (the lower part of Fig. 1 a) the resistivity decreases and demonstrates the metallic-like behaviour. The magnitude of the drop in resistivity, $(\rho_{\text{high}} - \rho_0)/\rho_0$, obviously depends on the disorder and varies from a factor of 5 (the lowest curves in Fig. 1 a) to a few % in Fig. 1 c. As density decreases below a ‘critical value’ n_c , the character of the temperature dependence changes to the insulating one. The changes in the character of $\rho(T)$ at $n = n_c$ are reminiscent of a typical metal-insulator transition (MIT) in 3D

systems which is not expected to occur in 2D system. In agreement with earlier observations [3,5,18] the increase in disorder causes the drop in resistivity to weaken, the ‘critical’ density n_c to increase and the ‘critical’ resistivity ρ_c to decrease.

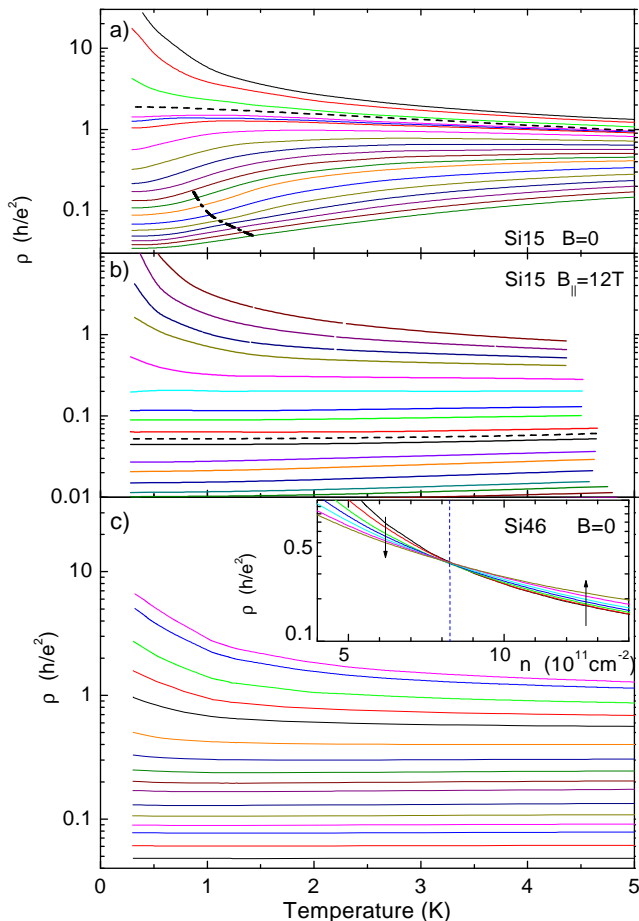


FIG. 1. T -dependence of the resistivity (a) for high mobility sample Si15 at $B = 0$, and (b) at $B_{\parallel} = 12T$; (c) for low-mobility sample Si46 at $B = 0$. Inset shows $\rho(n)$ for $T = 1, 2, 4, 8, 16, 32, 62$ K (arrows indicate direction of the growth in temperature). Horizontal dashed lines correspond to a ‘critical density’ n_c . Dash-dotted line in the panel (a) marks $T = 0.1T_F$. The densities (in units of 10^{11}cm^{-2}) on the panel (a) are 0.76, 0.79, 0.85, 0.89, 0.90, 0.91, 0.96, 1.01, 1.07, 1.12, 1.18, 1.23, 1.29, 1.40, 1.51, 1.62, 1.73, 1.84, 1.95; (b) 0.95, 1.07, 1.18, 1.29, 1.51, 1.73, 2.06, 2.28, 2.61, 2.94, 3.39, 3.72; and on the panel (c) 3.85, 4.13, 4.83, 5.53, 6.23, 7.63, 9.03, 10.4, 11.8, 13.2, 16.0, 18.8, 21.6, 24.4, 30.0, 37.0.

However, in contrast to the common believe that only high mobility samples are subject to the MIT, we demonstrate in the inset to Fig. 1 c that even for such low mobility sample as Si46, there is a clear crossing point, $n = n_c$, where $d\rho(T)/dT$ changes sign. The difference from that for high mobility samples (Fig. 1 a) is the shift of the events to much higher temperatures, to the range $T = 1 - 60K$, whereas for lower temperatures $T < 1K$

the weak localization upturn in the resistivity sets in. This upturn is a subject of more detailed consideration [13] and is not discussed here. The increase in the temperature scale by about 10 times as a function of disorder is anticipated since the Fermi energy, E_F , at the critical carrier density for disordered sample Si46 are 10 times bigger than that for Si15; correspondingly, in both samples the MIT is observed in similar ranges of (T/E_F) . Comparing Figs. 1 a and 1 c we arrive at the conclusion that the overall temperature dependence of the resistivity for Si-MOS samples may be roughly scaled by taking into account disorder dependence of the critical density n_c and the corresponding energy scale. We ignore at the moment a *disorder dependence of the strength in the resistivity drop*, which will be considered further.

II. THE EFFECT OF THE PARALLEL MAGNETIC FIELD ON CONDUCTION

A. Magnetic field driven MI-transition?

It was found in Refs. [17,18,23] that for a fixed carrier density an increase in B_{\parallel} causes $d\rho/dT$ to change sign. At first sight, this effect is reminiscent of a magnetic field driven transition; an analogy to the superconductor-insulator transition was discussed in Ref. [24] and the corresponding field value is often called ‘critical magnetic field’ B_c . In Figure 2 we reproduce similar behavior for n -Si-MOS samples.

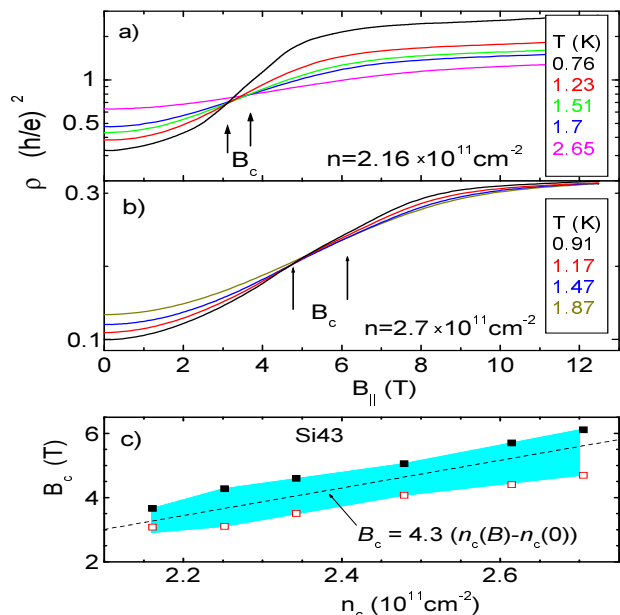


FIG. 2. a, b) Resistivity traces vs B_{\parallel} for different temperatures and for two densities. Sample Si43. Vertical arrows mark interval of fields which may be assigned to the ‘critical’ field value B_c . c) B_c vs carrier density. Shaded corridor corresponds to the interval of crossing. Dashed line is a linear fit.

Similar to that reported in Refs. [18,23,27], the $\rho(B)$ traces for different temperatures cross each other around a ‘critical’ magnetic field, B_c , though in an extended interval rather than in a single point. As carrier density n and magnetic field increase, the interval of crossing broadens and finally becomes infinite for $B \geq 6$ T. Density dependence of B_c is plotted in Fig. 2c in the range of fields where the crossing interval is finite.

In order to understand the driving mechanism of the magnetoresistance we performed more detailed studies of the magnetoresistance and measured its temperature dependence at various values of the in-plane field.

B. Analogy between the effects of parallel field and disorder on conduction

It is rather instructive to trace in detail the influence of the magnetic field on the density and temperature dependences of the resistivity. The most striking and known result of the in-plane magnetic field is the increase in the sample resistivity. Figure 3 demonstrates that the mobility degrades in magnetic field smoothly, without a threshold. Besides decreasing sample mobility, the magnetic field causes its maximum to shift to higher density. Both these effects are typical for the $B = 0$ case when the mobility is varied by changing the disorder; at low carrier density this is usually described in terms of the increase in the number of scatterers, $n_i \propto 1/\mu^{\text{peak}}$ [28].

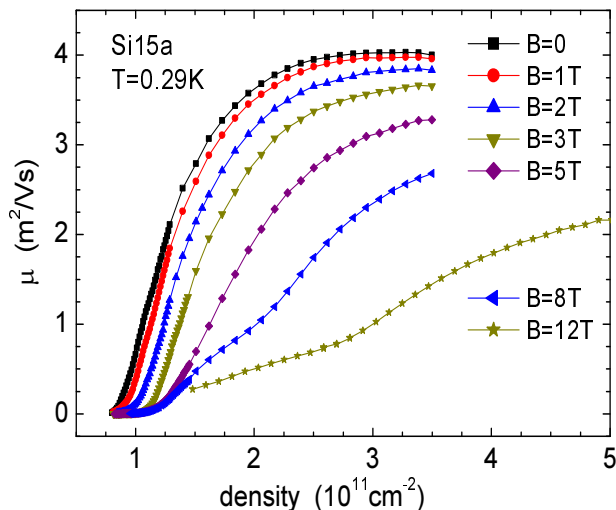


FIG. 3. Mobility vs carrier density for a fixed temperature $T = 0.29$ K and for different magnetic fields $B_{||}$ (indicated in the figure).

In Figures 4, we show the resistivity traces vs density for four fixed temperatures in the range 0.3 to 1 K. All four groups of curves for different $B_{||}$ values demonstrate a critical behaviour. The well defined crossing point or

‘critical’ density, n_c , separates regimes of temperature activated (i.e. ‘insulating’, $n < n_c$) and non-activated (‘metallic’, $n > n_c$) conduction [29].

The figures clearly demonstrate again that the parallel field progressively increases the critical carrier density n_c and decreases the corresponding critical resistivity value ρ_c . For magnetic fields $B_{||} > 6$ T (not shown), the crossing point spreads into a density interval, though still shifting to higher densities. This is typical for *low mobility samples and typical for the effect of the disorder*.

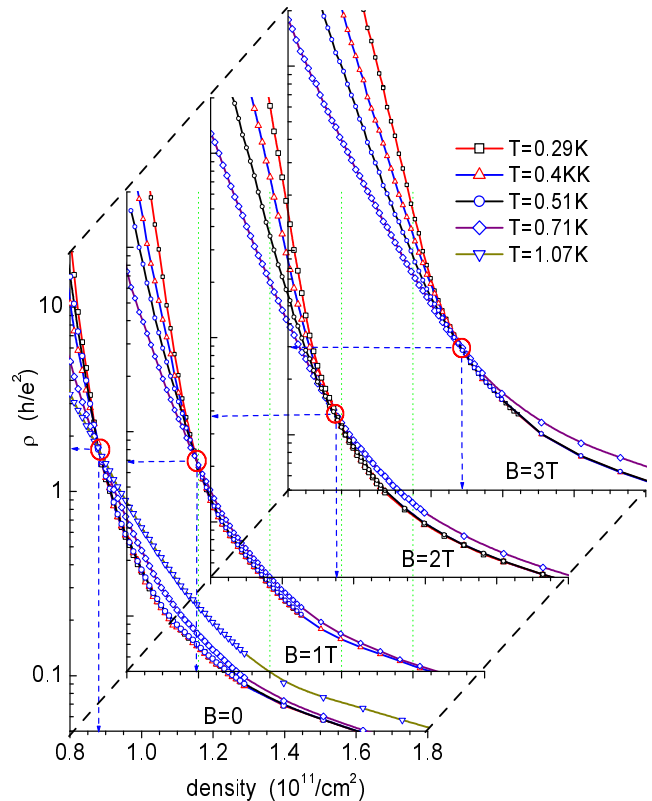


FIG. 4. Resistivity vs carrier density for 4 fixed temperatures (indicated on the figure) measured at $B_{||} = 0, 1, 2$ and 3 Tesla. Arrows at each panel mark the critical density and resistivity.

From Figure 4, we determined the coordinates of the crossing point, n_c and ρ_c , for each $B_{||}$ value and plotted them in Figs. 5. These two curves $n_c(B)$ and $\rho_c(B)$ have a transparent meaning: they separate the regimes of the temperature activated and ‘non-activated’ conduction on the planes $\rho(B, n)$ [29]. We find again that both field dependences are qualitatively similar to the ones known for the action of disorder (e.g., inverse sample peak mobility $1/\mu$, or $1/k_F l$ value) [3,5,18].

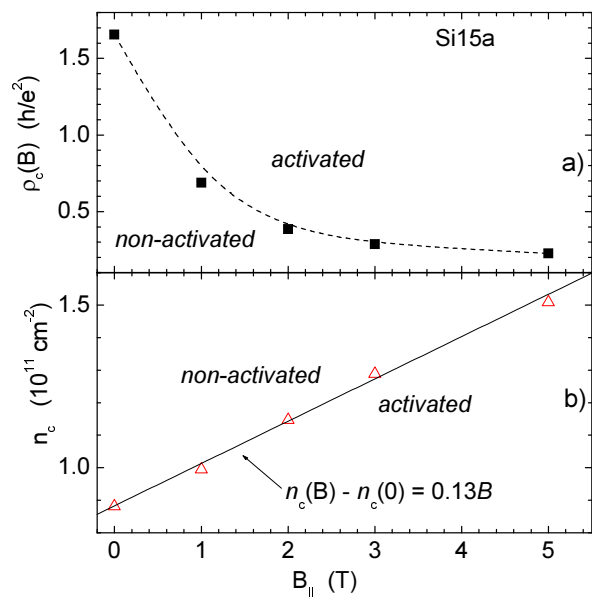


FIG. 5. Critical resistivity (a) and critical carrier density (b) vs parallel magnetic field. Full line is a linear fit with adjustable slope and with $n_c = 0.883 \times 10^{11} \text{ cm}^{-2}$. Dashed line is a guide to the eye.

Figure 6 shows for comparison the $\rho_c(n_c)$ dependence measured with the sample Si15 in various parallel fields (calculated from Fig. 4) and $\rho_c(n_c)$ reproduced from Ref. [3] for different samples at $B = 0$. A clear analogy is seen between the decrease in ρ_c caused by disorder and magnetic field.

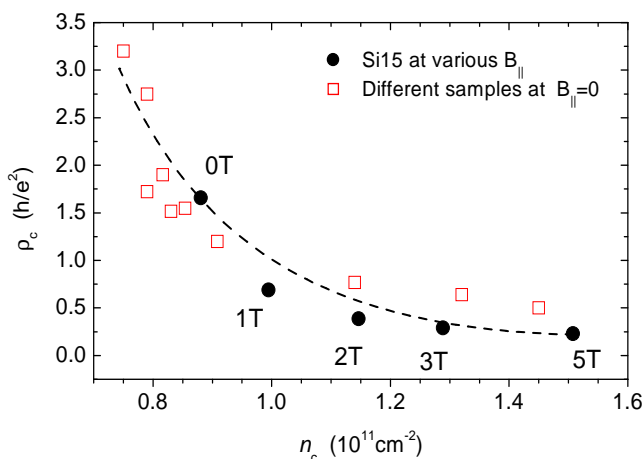


FIG. 6. “Critical” resistivity value vs “critical” density. Closed squares show the dependence driven by magnetic field, open squares are for the one driven by disorder (plotted for 9 different samples, based on the data from Ref. [3]). Line is the guide to the eye.

Finally, in order to illustrate the conclusion that the action of the magnetic field is similar to that of the disorder, we plotted in Fig. 1 b, for comparison, $\rho(T)$ for the same high mobility sample Si15 but measured with applied parallel field of 12 T. In light of the above discus-

sion, the transformation of Fig. 1 a into Fig. 1 b can thus be treated as a result of a progressive increase in electron scattering introduced by the parallel magnetic field, in steps like those shown in Figs. 4 and 3. The similarity between Figs. 1 b and 1 c supports this conclusion.

C. Magnetoresistance in parallel field and the g -factor

A number of experimental studies (e.g., Refs. [19,20]) demonstrate that the parallel field magnetoresistance in Si-MOS samples is a spin rather than orbital effect. There were, consequently, a number of empirical attempts to extract the g^* -factor value from different features of the magnetoresistance $R(B_{\parallel})$. For comparison, we present in Fig. 7 the density dependences of two characteristic magnetic fields: B_{sat} , corresponding to the saturation of $R(B_{\parallel})$ (for Si15 and Si43) from Ref. [20], and the ‘critical magnetic field’ B_c (for Si15) re-plotted from Fig. 5.

First of all, it is clear, that B_{sat} does not depend solely on the carrier density, but does also depend on the disorder. Whereas the empirical dependences $B_{\text{sat}} = s(n - n_b)$ for different samples have almost the same slope s , the offset n_b was found to be inversely proportional to the sample mobility [20]. For different samples, n_b varies from $0.5n_c$ for the highest mobility sample Si9 to $0.7n_c$ for Si15, $0.8n_c$ for Si12, and $0.96n_c$ for Si43. On the other hand, the ‘critical field’ B_c , by definition, extrapolates to zero at $n = n_c(B_c)$. For this reason, the two curves, $B_{\text{sat}}(n)$ and $B_c(n)$ usually intersect. Obviously, n_b cannot be identified with n_c . At low densities, B_{sat} exceeds B_c and the saturation of the magnetoresistance takes place in the insulating regime. At higher densities, the saturation occurs in the ‘metallic’ regime; the borderline for the sample Si15 corresponds to $n = 1.75 \times 10^{11} \text{ cm}^{-2}$.

For comparison, the dashed-dotted line in Fig. 7 represents the calculated density dependence of the field corresponding to the complete *spin polarization of conducting electrons*:

$$B_{\text{pol}} = \frac{2E_F}{g^* \mu_B} = \left(\frac{h}{e} \right) \left(\frac{n}{g^* m^*} \right) \frac{2}{g_v}, \quad (1)$$

where the renormalized $g^* m^*$ -values for conducting electrons were directly measured in Ref. [30] as a function of the carrier density.

For a given density n , $B_{\text{sat}}(n)$ is usually *less* than the field of complete spin-polarization B_{pol} of the conducting electrons. The deficit, $B_{\text{pol}} - B_{\text{sat}}$, increases as sample mobility decreases [20]; for example, $B_{\text{pol}} - B_{\text{sat}} \approx 4 \text{ T}$ for Si43. Whereas B_{pol} is solely determined by the mobile carrier density, B_{sat} turns out to be also dependent on disorder.

For high mobility samples, over a certain range of densities (which is $(1.2 - 2.2) \times 10^{11} \text{cm}^{-2}$ for Si15) the two quantities, B_{pol} and B_{sat} , are rather close to each other. This coincidence is in a good agreement with the observation by Vitkalov et al. [19] who found that in the range of densities $n = (1.54 - 4.5) \times 10^{11} \text{cm}^{-2}$, the frequency of the Shubnikov-de Haas oscillations in tilted fields doubles at a field which is equal to B_{sat} to within 5%. However, for more disordered samples (such as e.g. Si43 in Fig. 7), the saturation occurs in magnetic fields essentially lower than the polarization field B_{pol} , because of the twice as large n_b value (data on n_b for a number of samples may be found in Ref. [20]). We believe therefore that the coincidence of B_{sat} and B_{pol} for some high mobility samples and in a limited density range is rather occasional.

In the analysis of the $B_{\text{sat}}(n)$ -data in Ref. [31], it was assumed that B_{sat} remains equal to B_{pol} in the $n \rightarrow n_c$ limit. With this assumption authors arrived at the conclusion that g^* diverges as the density decreases, and that a ferromagnetic transition takes place at the MIT. As Fig. 7 shows, the coincidence of B_{sat} and B_{pol} fails for densities lower than $1.3 \times 10^{11} \text{cm}^{-2}$ (even for the high mobility sample). The g^* -factor for conducting electrons measured in Ref. [30] from Shubnikov-de Haas effect does not diverge at n_c , but gradually grows as the density decreases; the growth is anticipated within the Fermi-liquid theory [25,26].

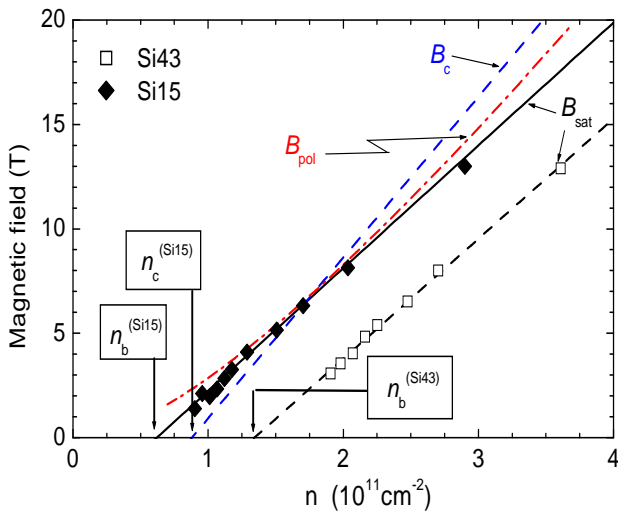


FIG. 7. B_c and B_{sat} for the sample Si15 (full diamonds) and B_{sat} for Si43 (empty squares) measured in the range $B_{\parallel} = 1.3 - 13 \text{T}$ and extrapolated schematically over a wider range of B_{\parallel} . B_{pol} is the field for complete spin polarization of the *conducting electrons*, calculated according to Eq. (1) and using $g^*m^*(n)$ values measured in Ref. [30].

One might conclude that the non-zero value of n_b is the only reason for the difference between B_{sat} and B_{pol} , and that by subtracting n_b the two parameters may be brought into agreement. However, such procedure performed in Ref. [20] for different samples, has

revealed that the two parameters are indeed related to different physics: the $(gm)_{\text{MR}}$ values estimated from the magnetoresistance either as $(h/e)n/B_{\text{sat}}$, or $(h/e)(n - n_b)/B_{\text{sat}}$ disagree with the $(g^*m^*)_{\text{SdH}}$ -values measured from Shubnikov-de Haas effect. This is also seen in Fig. 7 where (i) at low densities the difference between the measured $B_{\text{sat}}(n)$ values and the $B_{\text{pol}}(n)$ curve can not be eliminated by a horizontal shift (i.e., by varying n_b) and (ii) the slopes of the $B_{\text{sat}}(n)$ and $B_{\text{pol}}(n)$ curves are different.

We now consider another characteristic field, B_c . In Ref. [27], the $B_c(n_c)$ -dependence for 2D holes in (311)GaAs was noted to correspond to such spin alignment in the 2D carrier system where the spin-minority population drops below a threshold (which is approximately independent of the total 2D hole density or the magnetic field); the latter is of the order of the critical density at zero field $n_c(B = 0)$ [27]. In order to verify such possibility for Si-MOS samples, we fitted in Fig. 5 b the $n_c(B)$ data for the high mobility sample Si15 with a linear dependence $n_c(B) - n_b = cB$, with two adjustable parameters n_b and c . We find that the offset, n_b , is indeed equal to the anticipated value $n_c(B = 0) = n_c$ (for sample parameters, see Table 1), however, the slope $c = 0.13 \times 10^{11} \text{cm}^{-2}/\text{T}$, disagrees with such interpretation. With this interpretation, the slope $c = dn_c/dB_c$ would be equal to $(g^*m^*)g_v e/2h$ (where $g_v = 2$ for n -(100)-Si); we obtain then $(1/2)(g^*m^*)_{\text{MR}} = 0.27$ over the displayed range of densities $n = (0.9 - 1.5) \times 10^{11} \text{cm}^{-2}$. We repeated the same procedure with the data from Fig. 2 b and found, correspondingly, $(1/2)(g^*m^*)_{\text{MR}} \approx 0.48$ for the range $n = (2.2 - 2.7) \times 10^{11} \text{cm}^{-2}$.

The increase in the slope, dB_c/dn with carrier density would mean the decrease of g^*m^* for lower densities. Such decrease contradicts the results of direct measurements of the $(g^*m^*)_{\text{SdH}}$ for *conducting electrons* from Shubnikov-de Haas effect [17,30]; the contradiction indicates that the slope of the $B_c(n_c)$ -dependence in Si-MOS samples might have a more complex interpretation [20,30].

Earlier [20] we concluded that the saturation of the magnetoresistance (MR) for Si-MOS samples in parallel field B_{sat} is more related to the g^* -factor of *localized electrons* than that of the *conducting ones*. We think the same is true for the magnetoresistance at $B = B_c$. To illustrate this conclusion, we compare in Table II the g^*m^* values (i) directly measured for mobile electrons from Shubnikov-de Haas effect [30], (ii) the data which follow from the slope, (dn_c/dB_c) , of the curves in Figs. 2 and 5, and (iii) the ones which follow from the slope (dn/dB_{sat}) of the density dependence of the saturation field [20].

At $r_s = 5.3$, the g^*m^* values determined from Shubnikov-de Haas oscillations and from MR in parallel field are comparable. However, at $r_s = 7.6$ they differ by a factor of two: g^*m^* determined from the SdH effect

increases with r_s as expected for conducting electrons [30]; in contrast, $(g^*m^*)_{B_c}$ and $(g^*m^*)_{B_{\text{sat}}}$ are close to the value $2m_b$ ($m_b = 0.19$ is the bare band mass) anticipated for the localized electrons.

TABLE II. Comparison of the (g^*m^*) and g^* measured from Shubnikov-de Haas effect (labeled ‘SdH’) [30] with values estimated from the MR in parallel field. Label ‘ B_c ’ denotes the data derived from dB_c/dn_c , and label ‘ B_{sat} ’ denotes the data from dB_{sat}/dn [20].

r_s	$\frac{1}{2}(g^*m^*)_{\text{SdH}}$	$\frac{1}{2}(g^*m^*)_{B_c}$	$\frac{1}{2}(g^*m^*)_{B_{\text{sat}}}$
5.3	0.44	0.48	0.35
7.6	0.665	0.27	0.34

We close this section with a note that the attempts of describing B_{sat} and B_c in terms of the diverging g^* -factor [33,31], face with problems of explaining (a) why the ‘divergence’ takes place at progressively (and essentially) lower r_s values (i.e. higher n_c values) as disorder increases and (b) why the diverging g^* values are different from those measured in Shubnikov-de Haas effect. The comparison presented in this section illustrates a rather complex behaviour of the magnetoresistance in the parallel field; definitely, a thorough theoretical consideration is needed in order to use this effect for extracting the electron spin properties.

D. Comparing the effects of B_{\parallel} and temperature on conduction

We would like to point to the interesting similarity between the action of the parallel magnetic field and the temperature on the resistivity. Figure 8 demonstrates that for sufficiently high carrier density, $n \gg n_c$, the application of high magnetic field increases resistivity by about 5-6 times and restores nearly the same zero-field ‘Drude’ resistivity value as the temperature does: i.e. $\rho(B > B_{\text{sat}}, T \ll T_F) = \rho(B = 0, T \gtrsim T_F)$. The similarity between the effect of the field and temperature holds only while conduction remains ‘non-activated’ (cf. Figs. 5).

The dashed line in Fig. 8 b, depicts the boundary (same as in Fig. 4) between the temperature-activated and ‘non-activated’ transport regimes. When the carrier density becomes lower than $n_c(B_{\text{max}})$ but is still bigger than $n_c(B = 0)$, the parallel field drives resistivity through this boundary at some field $B_c(n)$. As a result, the conduction mechanism in magnetic field changes and the similarity between Figs. 8 a and 8 b breaks. For this reason, the uppermost curves in Fig. 8 b show much bigger increase in the resistance with field than with temperature [32]. It is noteworthy, that at low density, the magnetoresistance saturation takes place in the activated

regime, at $B_{\text{sat}} > B_c$, whereas at higher density the saturation occurs in the ‘non-activated’ metallic regime (see Fig. 7).

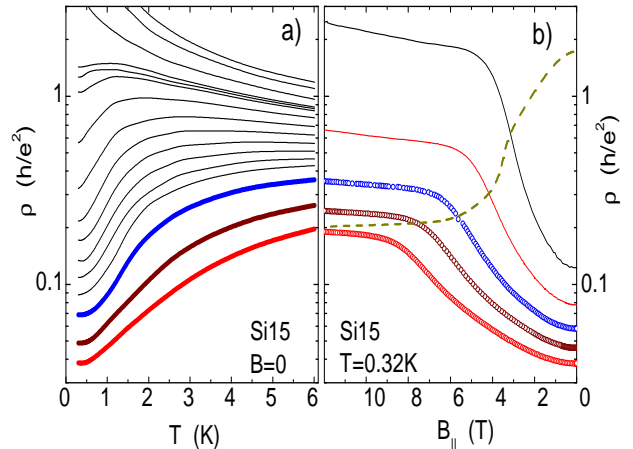


FIG. 8. Resistivity vs temperature (left panel) and parallel field (right panel) for different densities. Dashed line indicates the boundary for activated/nonactivated regime. On the left panel the densities are, from bottom to top: 1.84, 1.62, 1.40, 1.29, 1.23, 1.18, 1.12, 1.07, 1.01, 0.96, 0.91, 0.90, 0.89, 0.85, 0.79, $0.76 \times 10^{11} \text{cm}^{-2}$.

For the same reason, a very low magnetic field may be sufficient to drive the conduction from ‘non-activated’ to the ‘activated’ regime if the density n is chosen slightly less than n_c . In other words, this may be observed when $\rho(B = 0)$ is chosen very close to but less than $\rho_c(B = 0)$ (see Figs. 5 a and 8 b). In light of this note the destruction of the metallic conduction in ‘arbitrary small field’ [15] and the (B_{\parallel}/T) scaling of the resistivity at high ρ reported in Ref. [15] obtain a transparent interpretation [32].

E. Magnetic field driven disorder

It was verified experimentally [19,20] that in Si-MOS structures the parallel field couples to the electron spins only. Our results, therefore relate the action of the spin polarization and the increase in disorder. This may occur for example (i) via weakening of the screening in magnetic field [35], (ii) due to inter spin-subband scattering [36–38,27], or (iii) via increase in the Coulomb scattering caused by ‘undressing’ (i.e. depopulation and charging) of filled interface traps in any model of the interface traps [39–42].

As we demonstrate further, with the only assumption on the *disordering role of the parallel magnetic field*, we obtain a qualitative description of all presented data. We use this assumption as a phenomenological model; although we are unable to distinguish which one (or a combination) of the microscopic mechanisms is responsible for the parallel field magnetoresistance, we evaluate

various options in comparison with the data.

The similarity between the $\rho(T)$ - and $\rho(B_{\parallel})$ -traces in Fig. 8 seems easy to explain with the mechanism of screening which is temperature- [43–45] and magnetic field-dependent [35]. However, comparing this mechanism with the data we find a number of principle disagreements:

- a) The magnitude of the magnetoresistance (factor of 5 - 5.5 in Fig. 7 in the ‘metallic’ range) is larger than the screening mechanism can provide [35].
- b) At sufficiently high parallel field, $B > B_{\text{sat}}$, magnetoresistance almost saturates; this field was shown to be very close to the complete spin polarization of 2D carriers [19]. For the screening mechanism, even though the spin system is polarized, the temperature dependence of resistivity should be as strong as in zero field. The dashed line in Fig. 1 b corresponds to the density $n(B_{\text{sat}})$ at which the magnetoresistance for this sample saturates. Obviously, $\rho(T)$ depends on temperature much weaker than that in Fig. 1 a for $B = 0$.
- c) The Hall resistance data [38] also does not support the screening mechanism.

Last but not least: in Ref. [22] a deviation of the weak field Hall resistance from its classical value, was observed close to the critical density, particularly, on the ‘metallic’ side. This means that for n close to n_c there arises an excess or deficit of delocalized carriers; this observation obviously supports the latter scenario (iii). For this mechanism to work, the filled traps (or localized carriers, which is the same for us) should lift in energy with parallel field. This may take place for example, if the relevant traps form the upper Hubbard band [41], or if the traps are easy or spontaneously spin-polarized. We considered the latter possibility in Ref. [20] in order to explain *the disorder dependence of the field for saturation of the magnetoresistance*. We note that the spin polarization of localized states is favored by the broken inversion symmetry of the interface.

Interface defect charges originating from the lack of stoichiometry are intrinsic to Si/SiO₂ system; their typical density is 10^{12}cm^{-2} for a thermally grown dioxide [46]. As parallel field increases, the band (or upper band) of localized carriers should lift in energy and gets ‘undressed’ after passing through the Fermi energy. This will cause ‘turning-on’ the charged scatterers and corresponding increase in the scattering rate of the mobile carriers.

The carriers released from the traps will join the conduction band and may be detected via a deviation in the Hall voltage as n approaches $n_c(B)$; the latter may be driven either by decrease in n or by increase in B_{\parallel} . The trapped charge apriori may be of arbitrary sign which depends on the interface chemistry and growing processing.

Consequently, the deviation in the Hall voltage may be of arbitrary sign as well. Whereas the contributions into the Hall voltage of the released electrons and holes may compensate each other, it is not the case for the spatially separated charged scatterers. The number of ‘turned-on’ scatterers N_i is therefore expected to be much bigger than the deviation in the Hall resistance. In Ref. [22], we observed dV_H/V_H of the order of $(1 - 10)\%$ in different samples for the carrier density $n \sim 10^{11}\text{cm}^{-2}$; from this figure a lower estimate for the number of ‘turned-on’ scatterers, $N_i \gg (10^9 - 10^{10})\text{cm}^{-2}$, follows.

It is noteworthy, the inter(spin)-subband scattering [36–38,27] is not an alternative option but may be supplementary to the mechanism of the magnetic field driven disorder and charged traps. However, recent experiments [30,56] have shown that the scattering times in different spin and valley-subbands in (100)-Si are close to each other even though the degree of polarization is $\sim 30\%$. This sets substantial constraints on those two-band models which imply the intra-subband scattering times to be different.

For completeness, we mention that the parallel field magnetoresistance in Si-MOS samples was measured earlier by Bishop, Dynes and Tsui [47] and by Burdis and Dean [48] (though as a weaker effect on more disordered samples) and associated with electron-electron interaction and Zeeman splitting [49]. In this interpretation, however, the values of the interaction constant F were found to be unomalously large and to *decrease as temperature decreases* [48] which is not consistent with theoretical expectations. We obtained qualitatively similar results on high mobility samples [50,51]. In other words, $\rho(B_{\parallel}, T)$ in the ‘metallic’ range *does not scale* as a function of (B/T) which is expected for the Zeeman term $\delta\sigma = -0.084(F/2)(g^*\mu_B B/k_B T)^2$ [49]. It seems therefore unlikely the strong magnetoresistance in Si-MOS samples to be caused by electron-electron interaction.

We limited our consideration by strong changes in resistivity, $\delta\rho(B)/\rho \sim 1$. Parallel magnetic field causes an additional small effect on the quantum corrections to the conductivity, by decreasing the phase breaking length [51]; the latter though does not contradict our concept of the magnetic field driven disorder.

III. IMPLEMENTATION OF THE MODEL FOR ANALYSIS OF OTHER DATA

In order to verify the above model we compared it with all available data for Si-MOS sample and found rather good agreement. For the sake of shortness, we present here the comparison only with those data for which it was explicitly stated in Ref. [34] that “the enormous response observed at low temperatures is a consequence of effects other than parallel magnetic field-induced changes in carrier density or disorder strength”.

A. Example 1.

We begin with results obtained by Shashkin et al. and reproduce them from Fig. 9 of Ref. [34]. These data shown in Fig. 9 “dramatically demonstrate an extreme sensitivity of the resistance to parallel field” at $T = 30$ mK. The localized behaviour which appears to be absent for the curve at $B = 0$ is restored in a magnetic field” (cited from Ref. [34]). Based on this contrast it was stated in Ref. [34] that the effect of the parallel field is something different from the increase in disorder.

We plot in Fig. 9 the model curves using a conventional temperature activated dependence

$$\rho(T) = \rho_0 + \rho_1 \exp(\Delta/T). \quad (2)$$

The effect of the magnetic field in our model is presented in the magnetic field dependence of the activation energy $\Delta(B_{\parallel}) \equiv \Delta(n - n_c(B_{\parallel}))$. We fitted the curves to the data using three adjustable parameters ρ_0 , ρ_1 and Δ ; their numerical values are indicated on the figure. Whereas there is a certain correlation between ρ_0 and ρ_1 , we focus on the activation energy Δ which is well defined and almost independent of other parameters.

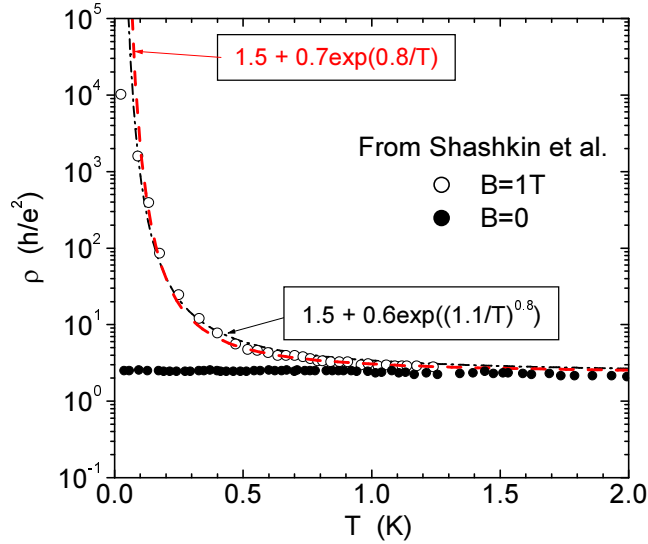


FIG. 9. a) Resistivity of Si-MOS sample vs temperature at zero field and at $B_{\parallel} = 1$ T. Density $n = 0.75 \times 10^{11} \text{ cm}^{-2}$. Reproduced from Fig. 9 of Ref. [34]. Dashed and dash-dotted curves are fitting dependences.

The carrier density $n = 0.75 \times 10^{11} \text{ cm}^{-2}$ is set equal to the critical density, $n = n_c(B = 0)$. By definition, the almost horizontal curve for $B = 0$ corresponds to $\Delta = 0$. Fitting the upper curve we obtained $\Delta_{fit} = 0.8$ K which is reasonably consistent with a value calculated on the basis of our results from Fig. 5: $\Delta_{calc} = (d\Delta/dn)[n - n_c(B = 1T)] = 0.6$ K. For this estimate we used the coefficient $d\Delta/dn = (4 - 5)$ [K

10^{-11} cm^2] measured earlier [52] for variety of high mobility samples. The lowest temperature point deviates substantially from the fitting curve; we presume this is due to either electron overheating by ~ 0.07 K [53] or by a crossover to another T -dependence. We also didn't care about a minor discrepancy for $T > 1.5$ K; this may be eliminated by a simple modification of the model as demonstrated further.

Anyhow, the increase in the measured resistivity by four orders of magnitude (which authors of Ref. [34] considered as an extraordinary effect) is at least 10 times smaller than the increase demonstrated by the conventional exponential dependence Eq. (1) (dashed curve). In general, the model curve fits the data rather well and some further improvement may be obtained by varying the critical index; an example is illustrated in Fig. 8 by the dash-dotted curve and the lower formula. The success of this fitting, as well as the consistency between the calculated and fitted values for Δ confirm that the action of the magnetic field is simply described by the increase in the critical density value $n_c(B)$ related to the magnetic field induced disorder.

B. Example 2

We now turn to the data by Simonian et al. [15] and reproduce them in Fig. 10 a; it shows the temperature dependence of ρ for Si-MOS sample measured in fixed various in-plane fields between 0 and 1.4 T. The data were discussed in Ref. [34] as a demonstration of an abrupt onset of the metallic behaviour and abrupt development of the magnetoresistance.

We note first that the overall $\rho(T)$ behavior for this sample is different from that shown in Fig. 9: here is no room for a temperature independent curve in the range $2 \text{ K} > T > 0.2 \text{ K}$ and the ‘separatrix’ $\rho(T, n = n_c)$ is tilted [53]. Correspondingly, the resistivity curves for this sample plotted vs density, for various temperatures (in the range (0.2-2) K) *would not cross each other at a single density* [54].

The carrier density $n = 0.883 \times 10^{11} \text{ cm}^{-2}$ in Fig. 9 a was set close to n_c so that the effect of the field is large. Initially, at $B_{\parallel} = 0$, the resistivity demonstrates a ‘metallic’ temperature dependence typical for high mobility Si-MOS samples (cf. Fig. 1 a), but as field increases, it transforms to a typical ‘insulating’ one. We estimate the transition between ‘metallic’ and ‘insulating’ behaviour to occur in the region marked with a horizontal arrow, $n_c(B = 0.93 T) = n$. From this number and using the empirical dependence $n_c(B)$ from Fig. 5 we estimated the critical density at zero field, $n_c(B = 0) = 0.76 \times 10^{11} \text{ cm}^{-2}$; this agrees within 5% with the number (0.802) given in Ref. [15].

We fitted all curves first with the exponential dependence $\rho = \rho_0 + \rho_1 \exp(\frac{\Delta}{T})$, same as Eq. (2). For the

‘metallic’ region (curves 1, 2, 3), this empirical dependence with $\Delta < 0$ is known to describe $\rho(T)$ for different samples [37,53,13]. For the ‘insulating’ region (curves 4, 5, 6), Eq. (2) with $\Delta > 0$ has a meaning of the temperature-activated dependence (though the same might be done with a variable-range hopping exponent). The three adjustable parameters, Δ , ρ_0 and ρ_1 , were fitted for each curve; their values are given in Table 2. We found the fit is rather good for low temperatures, $T < 2$ K.

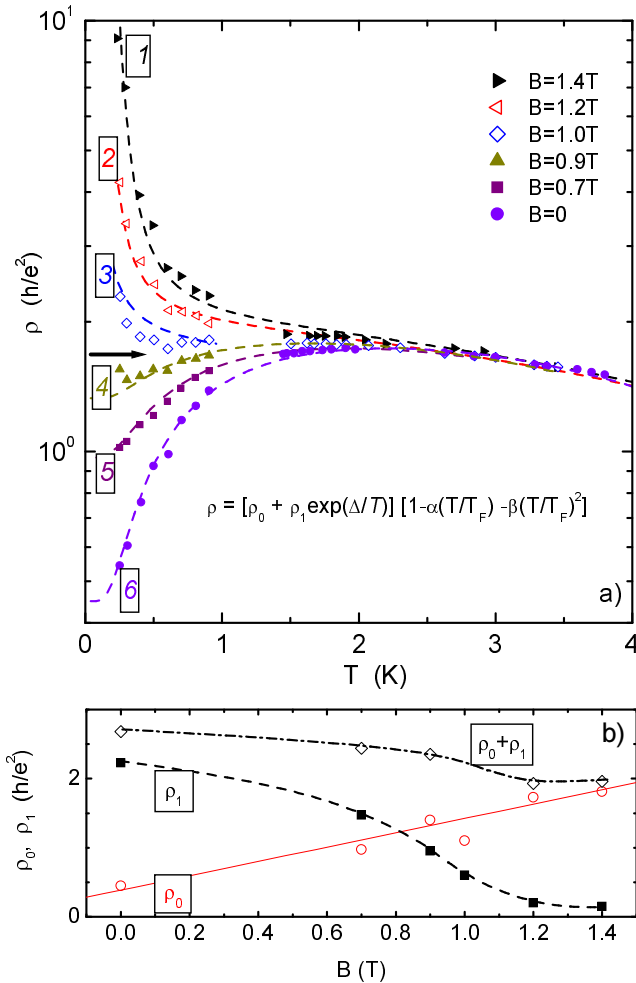


FIG. 10. a) Resistivity vs temperature for different fixed parallel fields (shown at the top). Dashed lines show fitting curves in the insulating range (curves 1, 2, 3) and metallic range (curves 4, 5, 6). Horizontal arrow marks an estimated location of the ‘critical’ trace. b) Two fitting parameters vs parallel field. Experimental data are reproduced from Ref. [15]

Eq. (1) can not obviously describe the high temperature region $T > 2$ K, therefore we also applied a modified expression which takes into account the non-exponential ‘tilt’ of the experimental data:

$$\rho = \left(\rho_0 + \rho_1 \exp\left(\frac{\Delta}{T}\right) \right) \left(1 - \alpha \frac{T}{T_F} - \beta \left(\frac{T}{T_F} \right)^2 \right). \quad (3)$$

The two additional parameters $\alpha = 0.194$ and $\beta = 0.46 - 0.66$ are uncorrelated with the other ones, and are directly obtained from the tilt at high temperatures.

Figure 10 shows that Eq. (3) fits the data rather well over the whole range of T whereas for low temperatures, $T < 2$ K, both fits, with Eqs. (2) and (3), are almost indistinguishable. The resulting parameters for both fits are given in Tables 2, and 3, correspondingly. Comparing the fitting curves with data, we conclude that the ‘abrupt changes’ discussed in Ref. [34] are nothing more than just a conventional exponential dependence.

The field dependence of the two principle parameters, ρ_0 and ρ_1 is shown in Fig. 10 b: ρ_0 increases with field demonstrating the disordering role of the field (though we don’t think that the almost linear increase is a universal feature for different samples). The strength of the ‘resistance drop’ in the ‘metallic’ range, $(\rho_0 + \rho_1)/\rho_0$, decays with field, also similar to the decay induced by disorder [3,55]. The critical resistivity, ρ_c , in our model is given by the sum $\rho_0 + \rho_1$; we find a qualitative similarity between the two independently calculated curves, $\rho_c(B)$ in Fig. 5 and $\rho_0 + \rho_1$ vs B in Fig. 10 b.

TABLE III. Parameters of the six curves for the fit with Eq. (1). n_c is in 10^{11} cm^{-2} , ρ_0, ρ_1 are in h/e^2 , and Δ is in K.

curve	B (T)	$n_c(B)$	ρ_0	ρ_1	Δ_{fit}	Δ_{calc}
1	1.4	0.945	1.45	0.24	1	0.31
2	1.2	0.919	1.29	0.35	0.6	0.18
3	1.0	0.893	1.09	0.6	0.2	0.05
4	0.9	0.881	1.0	0.8	-0.15	-0.01
5	0.7	0.855	0.9	1.1	-0.55	-0.14
6	0	0.765	0.45	2	-0.71	-0.59

TABLE IV. Parameters of the six curves shown in Fig. 10 for the fit with Eq. (2).

curve	B (T)	Δ_{fit}	ρ_0	ρ_1
1	1.4	1.0	1.82	0.15
2	1.2	0.6	1.76	0.2
3	1.0	0.2	1.1	0.6
4	0.9	-0.75	1.4	0.95
5	0.7	-0.76	0.97	1.47
6	0	-0.75	0.45	2.23

For the curve 3, the fit is not perfect because it oscillates vs temperature, which is beyond the frameworks of the model. The only steep feature may be found in the field dependence of ρ_1 at the transition from insulating to metallic behavior; this however may be caused by a minor mismatching of the oversimplified model curves in the metallic and insulating ranges.

The ‘activation energy’ Δ depends on the choice of the model and on average is 2-3 times larger than the values estimated from Fig. 5 (cf. the right columns in Table 2). This discrepancy is presumably caused by the admixture to the data of a non-exponential temperature dependence which is essentially strong for the considered sample and which can not be separated at low temperatures from the exponential one. For example, we were able to achieve a reasonable fit of the data with Eq. (2), using the *calculated* in Table 2 values $\Delta_{\text{calc}} = (d\Delta/dB) \times (n_c - n)$ when we modeled the ‘tilted separatrix’ in Eq. (3) by a power law factor, T^{-p} , rather than by the polynomial factor.

In Ref. [34] it was stated that “the effect of magnetic field cannot be ascribed solely to a field-induced change in the critical electron density”. We verified this possibility and arrive at the opposite conclusion. The success of our fitting confirms that the action of the parallel field, at least, to the first approximation consists in progressive increase of disorder. This is described by increasing the T -independent scattering rate $\rho_0(B_{\parallel})$, decreasing the magnitude of the resistivity drop, $(\rho_1 + \rho_0)/\rho_0$, and increasing the critical carrier density $n_c(B_{\parallel})$; the three parameters are not independent and within the same material system may be reduced only to the single parameter, e.g. $n_c(B_{\parallel})$.

IV. SUMMARY

To summarize, the results reported in this paper demonstrate that the effect of the parallel magnetic field on resistivity in high mobility Si-MOS samples (though via Zeeman coupling) is similar to that of disorder and, to some extent, to that of temperature. In other words, *parallel magnetic field increases disorder*. The temperature dependence of resistivity for various disorder and magnetic fields may be reduced to the dependences of the ‘critical’ density n_c on magnetic field and on disorder; the changes in the resistivity drop with temperature, $(\rho_0 + \rho_1)/\rho_0$, caused by disorder and magnetic field may be also mapped onto each other. We find a similarity between the action of the parallel field and temperature for the region of carrier density and field where conduction remains ‘non-activated’. These findings set constraints on the choice of the developed microscopic models.

The analogy between the parallel field and disorder points to the existence of a sub-band of localized carriers. Such band of localized carriers should lift in energy as a function of the parallel field, gets ‘undressed’ after passing through the Fermi energy and cause the increase in the scattering rate. The strong evidence for this mechanism is the variation in the Hall voltage observed in the vicinity of the metal-insulator transition. We can not exclude also the contribution of the inter spin-subband scattering, as a complementary feature to the above mechanism. However, our Shubnikov-de Haas

data [30,56] indicates that the mobility in different spin and valley sub-bands of conducting electrons are almost equal and the intersubband scattering does not play a major role in the temperature- and parallel field- dependence of the resistance. Applying the model of a field dependent disorder, we find a qualitative explanation of the whole set of presented results.

V. ACKNOWLEDGEMENTS

One of the authors (V.P.) acknowledges hospitality of the Lorenz Centre for theoretical physics at Leiden, where part of this work was done and reported at the workshop in June, 2000. The work was supported by NSF DMR-0077825, Austrian Science Fund (FWF P13439), INTAS (99-1070), RFBR (00-02-17706), the Programs ‘Physics of solid state nanostructures’, ‘Statistical physics’, ‘Integration’ and ‘The State support of the leading scientific schools’.

-
- [1] S. V. Kravchenko, G. V. Kravchenko, J. E. Furneaux, V. M. Pudalov, and M. D’Iorio, Phys. Rev. B **50**, 8039 (1994); S. V. Kravchenko, G. E. Bowler, J. E. Furneaux, V. M. Pudalov, and M. D’Iorio, Phys. Rev. B **51**, 7038 (1995).
 - [2] D. Popović, A. B. Fowler, S. Washburn, Phys. Rev. Lett. **79**, 1543 (1997). P. T. Coleridge, R. L. Williams, Y. Feng, P. Zawadzki, Phys. Rev. B. **56**, R12764 (1997). A. R. Hamilton, M. Y. Simmons, M. Pepper, E. H. Linfield, P. H. Rose, and D. A. Ritchie, Phys. Rev. Lett. **82**, 1542 (1999).
 - [3] V. M. Pudalov, G. Brunthaler, A. Prinz, and G. Bauer, a): JETP Lett., **68**, 442 (1998); b): Physica E, **3**, 79 (1998).
 - [4] Y. Hanein, U. Meirav, D. Shahar, C. C. Li, D. C. Tsui, H. Shtrikman, Phys. Rev. Lett. **80**, 1288 (1998).
 - [5] Y. Hanein, D. Shahar, J. Yoon, C. C. Li, D. C. Tsui, and Hadas Shtrikman, Phys. Rev. B **58** R13338 (1998).
 - [6] Y. Hanein, D. Shahar, J. Yoon, C. C. Li, D. C. Tsui, and Hadas Shtrikman, preprint: cond-mat/9808251.
 - [7] M. Y. Simmons, A. R. Hamilton, M. Pepper, E. H. Linfield, P. D. Rose, and D. A. Ritchie, cond-mat/9910368.
 - [8] V. Senz, U. Dötsch, U. Gennser, T. Ihn, T. Heinzel, K. Ensslin, R. Hartmann, D. Grützmacher, Ann. Phys (Leipzig) **8**, 237 (1999). cond-mat/9903367.
 - [9] V. M. Pudalov, G. Brunthaler, A. Prinz, and G. Bauer, Phys. Rev. B **60**, R2154 (1999).
 - [10] A. R. Hamilton, M. Y. Simmons, M. Pepper, E. H. Linfield, P. D. Rose, D. A. Ritchie, Phys. Rev. Lett. **82**, 1542 (1999). cond-mat/9808108.
 - [11] G. Brunthaler, A. Prinz, G. Bauer, and V. M. Pudalov, preprint: cond-mat/0007230.

- [12] B. L. Altshuler, D. L. Maslov, V. M. Pudalov, Phys. Stat. Sol.(b) **218**, 193 (2000); cond-mat/9909353.
- [13] B. L. Altshuler, G. W. Martin, D. L. Maslov, V. M. Pudalov, A. Prinz, G. Brunthaler, G. Bauer, cond-mat/0008005.
- [14] V. M. Pudalov, G. Brunthaler, A. Prinz, G. Bauer, JETP Lett. **65**, 932 (1997).
- [15] D. Simonian, S. V. Kravchenko, M. P. Sarachik, V. M. Pudalov, Phys. Rev. Lett. **79**, 2304 (1997).
- [16] V. M. Pudalov, G. Brunthaler, A. Prinz, G. Bauer, Physica B **249-251**, 697 (1998).
- [17] T. Okamoto, K. Hosoya, S. Kawaji, A. Yagi, Phys. Rev. Lett. **82**, 3875 (1999). cond-mat/9906425.
- [18] J. Yoon, C. C. Li, D. Shahar, D. C. Tsui, M. Shayegan, Phys. Rev. Lett. **84**, 4421 (2000). cond-mat/9907128.
- [19] S. A. Vitkalov, M. P. Sarachik, T. M. Klapwijk, preprint cond-mat/0101196. S. A. Vitkalov, H. Zheng, K. M. Mertes, M. P. Sarachik, T. M. Klapwijk, preprint: cond-mat/0004201.
- [20] V. M. Pudalov, G. Brunthaler, A. Prinz, and G. Bauer, cond-mat/0004206.
- [21] S. Das Sarma, E. H. Hwang, Phys. Rev. Lett. **83**, 164 (1999).
- [22] V. M. Pudalov, G. Brunthaler, A. Prinz, and G. Bauer, JETP Lett. **70**, 48 (1999). [Pis'ma ZhETF **70**, 48 (1999)].
- [23] M. Y. Simmons, A. R. Hamilton, M. Pepper, E. H. Linfeld, P. Rose, D. A. Ritchie, A. K. Savchenko, T. G. Griffiths, Phys. Rev. Lett. **80**, 1292 (1998). cond-mat/9808108.
- [24] P. Phillips, S. Suchdev, S. Kravchenko, and A. Yazdani, in Proc. Nat. Ac. Sci. USA, **96**, 9983 (1999).
- [25] A. A. Abrikosov, *Fundamentals of the Theory of Metals*, North-Holland, Amsterdam (1988).
- [26] A. Isihara, *Electron Liquids*, Springer-Verlag, Berlin (1997).
- [27] E. Tutuc, E. P. De Poortere, S. J. Papadakis, M. Shayegan, preprint: cond-mat/0012128.
- [28] A. Gold, Phys. Rev. Lett. **54**, 1079 (1985). A. Gold and W. Gotze, Phys. Rev. B **33**, 2495 (1986).
- [29] For the definition and discussion of the 'insulating' and metallic regimes see Ref. [53].
- [30] V. M. Pudalov, M. Gershenson, H. Kojima, N. Butch, E. M. Dizhur, G. Brunthaler, A. Prinz, and G. Bauer, cond-mat/0105081.
- [31] S. A. Vitkalov, H. Zheng, K. P. Mertes, M. P. Sarachik, and T. M. Klapwijk, preprint: cond-mat/0009454.
- [32] The magnetic field driven transition from non-activated to activated conduction regime causes a strong exponential magnetoresistance $\delta\rho(B) \propto \exp(-\Delta(B_{\parallel})/T)$, where $\Delta(B) \propto (B - B_c)$; therefore, $\rho(B_{\parallel})$ scales as $f((B - B_c)/T)$. A theoretical consideration see in Ref. [41].
- [33] A. A. Shashkin, S. V. Kravchenko, V. T. Dolgoplov, T. M. Klapwijk, preprint: cond-mat/0007402.
- [34] E. Abrahams, S. Kravchenko, M. P. Sarachik, cond-mat/0006055.
- [35] V. T. Dolgoplov, A. Gold, JETP Letters, **71**, 27 (2000).
- [36] S. S. Murzin, S. I. Dorozhkin, G. Landwehr and A. C. Gossard JETP Lett., **67**, 101 (1998).
- [37] V. M. Pudalov, JETP Lett. **66** 175 (1997). [Pis'maZhETF **66** 168 (1997)].
- [38] A. A. Vitkalov, H. Zheng, K. M. Mertes, M. P. Sarachik, T. M. Klapwijk, preprint: cond-mat/0008456.
- [39] T. M. Klapwijk, S. Das Sarma, Sol. St. Commun. **110**, 581 (1999).
- [40] B. L. Altshuler, D. L. Maslov, Phys. Rev. Lett. **83**, 2092 (1999).
- [41] V. I. Kozub, N. V. Agrinskaya, S. I. Khondaker, I. Shlimak, cond-mat/9911450. V. I. Kozub, N. V. Agrinskaya, cond-mat/0104254.
- [42] V. M. Pudalov, G. Brunthaler, A. Prinz, G. Bauer, B. I. Fouks, cond-mat/9907401.
- [43] S. Das Sarma and E. H. Hwang, cond-mat/9812216. Phys. Rev. Lett. **83**, 164 (1999).
- [44] F. Stern, Phys. Rev. Lett. **44**, 1469 (1980).
- [45] A. Gold and V. T. Dolgoplov, Phys. Rev. B **33**, 1076 (1986).
- [46] T. Hori, *Gate dielectrics and MOS ULSIs*, Springer-Verlag, Berlin, NY, (1997).
- [47] D. J. Bishop, R. C. Dynes, and D. C. Tsui, Phys. Rev. B **26**, 773 (1982).
- [48] M. S. Burdis, and C. C. Dean, Phys. Rev. B **38**, 3269 (1988).
- [49] P. A. Lee, T. V. Ramakrishnan, Rev. Mod. Phys. **57**, 287 (1985). C. Castellani, C. Di Castro, P. A. Lee, Phys. Rev. B **57**, R9381 (1998).
- [50] V. M. Pudalov, G. Brunthaler, A. Prinz, G. Bauer, Bull. APS, **44** (1), 1077 (1999). To be published elsewhere.
- [51] M. E. Gershenson, H. Kojima, V. M. Pudalov, L. Czapla, to be published elsewhere. Bull. APS **46** (1) part II, 1158 (2001). Talk Y16.9.
- [52] V. M. Pudalov, M. D. Iorio, S. V. Kravchenko, J. W. Campbell, Phys. Rev. Lett. **70**, 1866 (1993). See also Fig. 5 in: M. D'Iorio, V. M. Pudalov, S. G. Semenchinsky, Phys. Rev. B **46**, 15992 (1992).
- [53] B. L. Altshuler, D. L. Maslov, V. M. Pudalov, cond-mat/0003032. Physica E, **9** (2), 209 (2001).
- [54] For this reason, the smeared curves crossing in Figs. 2 and 4 can not be considered as a proof for the absence of MIT in parallel field.
- [55] V. M. Pudalov, G. Brunthaler, A. Prinz, G. Bauer, Physica E, **3**, 79 (1998).
- [56] V. M. Pudalov, A. Punnoose, G. Brunthaler, A. Prinz, G. Bauer, cond-mat/0104347.